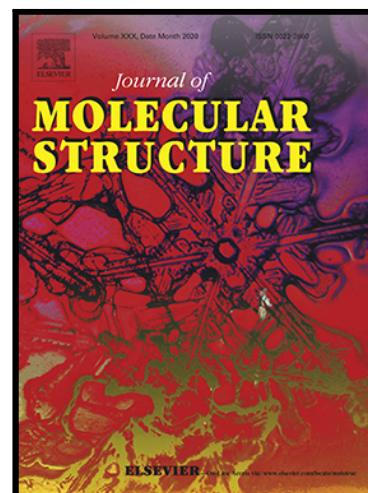


Journal Pre-proof

Reconnaissance of the reactions of carbamodithiolate salts with dialkyltin dichloride

Tushar S. Basu Baul , Maheswara Rao Addepalli , Andrew Duthie ,
M. Fátima C. Guedes da Silva

PII: S0022-2860(20)31856-1
DOI: <https://doi.org/10.1016/j.molstruc.2020.129541>
Reference: MOLSTR 129541



To appear in: *Journal of Molecular Structure*

Received date: 15 September 2020
Revised date: 27 October 2020
Accepted date: 28 October 2020

Please cite this article as: Tushar S. Basu Baul , Maheswara Rao Addepalli , Andrew Duthie ,
M. Fátima C. Guedes da Silva , Reconnaissance of the reactions of carbamodithi-
olate salts with dialkyltin dichloride, *Journal of Molecular Structure* (2020), doi:
<https://doi.org/10.1016/j.molstruc.2020.129541>

This is a PDF file of an article that has undergone enhancements after acceptance, such as the addition of a cover page and metadata, and formatting for readability, but it is not yet the definitive version of record. This version will undergo additional copyediting, typesetting and review before it is published in its final form, but we are providing this version to give early visibility of the article. Please note that, during the production process, errors may be discovered which could affect the content, and all legal disclaimers that apply to the journal pertain.

© 2020 Published by Elsevier B.V.

Highlights

- Reactions of carbamodithiolate salts with R_2SnCl_2 have been investigated.
- Four **new** complexes were characterized by IR, 1H , ^{13}C , and ^{119}Sn NMR spectroscopy.
- Complexes **1-4** and carbamodithiolate salts have been characterized by single crystal X-ray crystallography.
- X-ray analysis revealed two types of complexes with distorted square pyramid and skewed trapezoidal bipyramid geometry around tin atom.
- The 3D Hirshfeld surfaces have been mapped to study the intermolecular interactions.

Reconnaissance of the reactions of carbamodithiolate salts with dialkyltin dichloride

Tushar S. Basu Baul,^{a,*} Maheswara Rao Addepalli,^a Andrew Duthie,^b M. Fátima C. Guedes da Silva^{c,*}

^aCentre for Advanced Studies in Chemistry, North-Eastern Hill University, NEHU Permanent Campus, Umshing, Shillong 793 022, India

^bSchool of Life & Environmental Science, Deakin University, Geelong, Victoria 3217, Australia

^cCentro de Química Estrutural, Complexo I, Instituto Superior Técnico, Universidade de Lisboa, Av. Rovisco Pais, 1049-001 Lisboa, Portugal

ABSTRACT

Reactions of carbamodithiolate salts viz., $\text{c-C}_3\text{H}_6\text{NH}_3^+(\text{L}^1)^-$ and $\text{c-C}_6\text{H}_{12}\text{NH}_3^+(\text{L}^2)^-$ ($\text{L}^1 =$ cyclopropylcarbamodithioate, $\text{L}^2 =$ cyclohexylcarbamodithioate) with R_2SnCl_2 ($\text{R} = \text{Me}$ or $n\text{-Bu}$) were investigated in dichloromethane for the first time. A series of four diorganotin(IV) complexes of composition $[\text{Me}_2\text{Sn}(\text{L}^1)\text{Cl}]$ (**1**), $[\text{Me}_2\text{Sn}(\text{L}^1)_2]$ (**2**), $[\text{Me}_2\text{Sn}(\text{L}^2)_2]$ (**3**) and $[n\text{-Bu}_2\text{Sn}(\text{L}^2)_2]$ (**4**) were isolated and characterized by spectroscopic methods. The structures of the two carbamodithiolate salts and the diorganotin(IV) compounds **1-4** were accomplished by X-ray crystallographic analysis revealing distorted square pyramid geometry for **1**, but skewed trapezoidal bipyramids for **2-4**. Influence of the carbamodithiolate moiety on the hydrogen-bond interactions and non-covalent contacts, as well as on the packing of the structures, is discussed. The 3D Hirshfeld surfaces were mapped and used to study the intermolecular interactions.

Keywords: diorganotin/ carbamodithiolate ligands/ spectroscopy/ crystal structure/ non-covalent contacts/ Hirshfeld surfaces

*Corresponding authors.

E-mail addresses: basubaul@nehu.ac.in, basubaulchem@gmail.com (T. S. Basu Baul), fatima.guedes@tecnico.ulisboa.pt (M. Fátima C. Guedes da Silva).

1. Introduction

Dithiocarbamic acids are excellent nucleophiles to a broad range of electrophiles, especially when derived from primary amines [1]. Although they are labile, their metal complexes and esters are stable and have found extensive applications e.g. as fungicides and pesticides [2], in vulcanization during rubber manufacturing [3], in polymerization reactions [4], as organic intermediates [5], in medicinal chemistry [6] and for the synthesis of metal sulfide nanoparticles [7]. Over the last few years significant attention has been paid to dithiocarbamate organotin chemistry and consequently organotin(IV) dithiocarbamates have reached a distinct pinnacle [8-10]. The strong Lewis acidity of tin, the presence of the anionic CS_2^- moiety in the dithiocarbamate ligand and the ease of synthesizing such complexes, led to the development of compounds of the type $[\text{R}_{4-n}\text{Sn}(\text{S}_2\text{CNR}'_2)_n]$ ($n = 1 - 4$) with a reasonable degree of predictability of the solid state structures for a given combination of R and R' [8]. Accordingly, a large number of such complexes were explored for the preparation of tin sulfide/ tin sulfide nanomaterials [11,12], photoluminescent materials [13], selective anion and ion receptors [14-16], fascinating architectures [15-19] and in biology [20-25], to mention some.

Although organotin(IV) compounds containing aromatic or aliphatic substituents at the dithiocarbamate fragment are abundant, those featuring a primary amine such as cyclopropylcarbamodithioate and cyclohexylcarbamodithioate are scarce except for a report by Jabbar *et al.* [26], wherein cyclohexylcarbamodithioic acid was isolated from a reaction of cyclohexylamine with carbon disulfide in ethanol. By following identical methodology we succeeded in the isolation and characterization of the carbamodithiolate salts *viz.*, $\text{c-C}_3\text{H}_6\text{NH}_3^+(\text{L}^1)^-$ and $\text{c-C}_6\text{H}_{12}\text{NH}_3^+(\text{L}^2)^-$ ($\text{L}^1 =$ cyclopropylcarbamodithioate, $\text{L}^2 =$ cyclohexylcarbamodithioate) and explored their synthetic potential towards diorganotin(IV)

dichloride. Report on the reactions of primary amine derived carbamodithioate salts with diorganotin(IV) dihalide are rare [27], although such reactions are known for secondary amines [28]. Additionally, it is known that the dithiocarbamates obtained from secondary amines are more stable than the products obtained from primary amines [29]. Here we report the preparations and isolation of diorganotin(IV) compounds *viz.*, [Me₂Sn(L¹)Cl] (**1**), [Me₂Sn(L¹)₂] (**2**), [Me₂Sn(L²)₂] (**3**) and [*n*-Bu₂Sn(L²)₂] (**4**) which were characterized by means of IR and NMR spectroscopy. The molecular structures of *c*-C₃H₆NH₃⁺(L¹)⁻ and *c*-C₆H₁₂NH₃⁺(L²)⁻ and **1-4** have been determined by single crystal X-ray crystallography (SCXRD).

2. Experimental

2.1. Materials and physical measurements

Dimethyltin dichloride (Sigma Aldrich), di(*n*-butyl)tin dichloride (Stream chemicals), cyclopropylamine, cyclohexylamine, carbon disulfide (Spectrochem), and ethanol (Merck) were used as received. The solvents used in the reactions were of AR grade and dried using standard procedures. Melting points were measured using a Büchi M-560 melting point apparatus and are uncorrected. Elemental analyses were performed using a Perkin Elmer 2400 series II instrument. IR spectra in the range 4000-400 cm⁻¹ were obtained on a Bruker Alpha-II FT-IR spectrophotometer with samples investigated as KBr discs (Figs. S1-S6). The ¹H and ¹³C spectra of compounds (carbamodithiolate salts and diorganotin(IV) compounds **1-4**, Figs. S7-S18) were recorded on a Bruker AMX 400 spectrometer and measured at 400.13 and 100.62 MHz, respectively. Solution ¹¹⁹Sn NMR spectra of compounds **1-4** were measured on a Jeol Zeta ECZ 400R spectrometer at 149.08 MHz (Fig. S19). ¹H, ¹³C and ¹¹⁹Sn chemical shifts were referenced to SiMe₄ (δ 0.00 ppm), CDCl₃ (δ 77.00 ppm), and Me₄Sn (δ 0.00 ppm), respectively.

2.2. Preparation of carbamodithiolate salts

Although reports on cyclopropanaminium cyclopropylcarbamodithioate [30] and cyclohexanaminium cyclohexylcarbamodithioate [31-33] are available in the literature, either the synthetic procedure or the characterization data is inadequate. Consequently, a general method has been developed which is described below.

2.2.1. Synthesis of cyclopropanaminium cyclopropylcarbamodithioate, $c\text{-C}_3\text{H}_6\text{NH}_3^+(\text{L}^1)^-$

Carbon disulfide (0.41 mL, 0.54 g, 7.15 mmol) was added dropwise to a stirred absolute ethanol solution (5 mL) of cyclopropylamine (1.00 mL, 0.82 g, 14.36 mmol) in a round bottom flask held at around 0 °C. Even though a pale-yellow precipitate was instantly formed the reaction mixture was allowed to gradually reach room temperature and the stirring was maintained for 4 h. The solid was then filtered, washed with small amount of ethanol and dried *in vacuo*. Pale-yellow crystals suitable for X-ray analysis were obtained upon slow evaporation of a methanolic solution of the product. Yield 1.1 g (84%). M.p.: 112-113 °C (109-111 °C [30]). Anal. found: C, 44.28; H, 7.62; N, 14.80. Calcd. for $\text{C}_7\text{H}_{14}\text{N}_2\text{S}_2$: C, 44.17; H, 7.41; N, 14.72%. ^1H NMR ($\text{CDCl}_3+\text{DMSO-}d_6$) δ_H (ppm): 7.76 (s, 1H, NH), 6.03 (bs, 3H, 3NH), 3.15-3.14 (m, 1H, CH), 2.58-2.54 (m, 1H, CH), 0.81-0.50 (m, 8H, 4CH₂). ^{13}C NMR ($\text{CDCl}_3+\text{DMSO-}d_6$) δ_c (ppm): 214.37 (C=S), 29.25 (CH), 22.74 (CH), 6.65 (CH₂), 4.19 (CH₂). IR absorption (cm^{-1}): 3222 (w), 3180 (s), 3086 (w), 2994 (m), 1645 (w), 1557 (s), 1512 (m), 1453 (w), 1403 (w), 1339 (m), 1274 (m), 1221 (w), 1200 (w), 1162 (w), 1047 (w), 1019 (w), 982 (m), 932 (w), 860 (w), 819 (w), 780 (w), 733 (w), 706 (w), 650 (w), 597 (w), 562 (w).

2.2.2. Synthesis of cyclohexanaminium cyclohexylcarbamodithioate, $c\text{-C}_6\text{H}_{12}\text{NH}_3^+(\text{L}^2)^-$

An analogous method to that used for the preparation of $\text{c-C}_3\text{H}_6\text{NH}_3^+(\text{L}^1)^-$ was followed using cyclohexylamine (1.00 mL, 0.86 g, 8.67 mmol) and carbon disulfide (0.25 mL, 0.33 g, 4.33 mmol). Colorless crystals suitable for X-ray analysis were obtained upon slow evaporation of a methanolic solution of the product. Yield 1.0 g (90%). M.p.: 182-183 °C (176-178 °C [30], 188-189 °C [31,32]), Anal. found: C, 56.68; H, 9.80; N, 10.02. Calcd. for $\text{C}_{13}\text{H}_{26}\text{N}_2\text{S}_2$: C, 56.88; H, 9.55; N, 10.21%. ^1H NMR ($\text{CDCl}_3+\text{DMSO}-d_6$) δ_H (ppm): 7.49 (s, 1H, NH), 5.93 (bs, 3H, 3NH), 4.17-4.15 (m, 1H, CH), 3.11-3.07 (m, 1H, CH), 2.07-1.10 (m, 20H, 10CH₂). ^{13}C NMR ($\text{CDCl}_3+\text{DMSO}-d_6$) δ_c (ppm): 210.80 (C=S), 55.16 (CH), 50.10 (CH), 31.83, 30.90, 25.05, 24.37, 23.96 (CH₂). IR absorption (cm^{-1}): 3316 (s), 2930 (s), 2855 (m), 1638 (m), 1481 (s), 1446 (w), 1389 (w), 1340 (m), 1251 (w), 1154 (w), 1120 (w), 1090 (w), 1014 (w), 980 (m), 943 (m), 886 (m), 795 (w), 664 (w), 639 (w), 559 (w).

2.3. Synthesis of diorganotin(IV) compounds **1-4**

2.3.1. Synthesis of $[\text{Me}_2\text{Sn}(\text{L}^1)\text{Cl}]$ (**1**)

Me_2SnCl_2 (0.10 g, 0.45 mmol) in dichloromethane (5 mL) was added dropwise to a stirred solution of $\text{c-C}_3\text{H}_6\text{NH}_3^+(\text{L}^1)^-$ (0.08 g, 0.44 mmol) also in dichloromethane (5 mL). After 4 h under stirring a white precipitate was formed which was isolated by filtration, washed with small amounts of dichloromethane and dried *in vacuo*. Crystals of **1** suitable for diffraction studies were obtained after several successive attempts of slow evaporation of dichloromethane solutions of the product. Yield: 0.09 g (62%). M.p.: 100-101 °C. Anal. found: C, 23.02; H, 4.03; N, 4.50. Calcd. for $\text{C}_6\text{H}_{12}\text{ClNS}_2\text{Sn}$: C, 22.77; H, 3.82; N, 4.43%. ^1H NMR (CDCl_3) δ_H (ppm): 7.89 (s, 1H, NH), 2.91-2.87 (m, 1H, CH), 1.32 (s, 6H, SnMe_2), 0.95-0.93 (m, 2H, CH₂), 0.87-0.81 (m, 2H, CH₂). ^{13}C NMR (CDCl_3) δ_c (ppm): 203.26 (C=S), 30.80 (CH), 10.25 (CH₂), 7.46

($^1J(^{13}\text{C}-^{119}\text{Sn})$ 566 Hz, SnMe_2). ^{119}Sn NMR (CDCl_3) δ_{Sn} (ppm): -158.4 . IR absorption (cm^{-1}): 3230 (s), 3038 (w), 1637 (m), 1536 (s), 1510 (s), 1397 (m), 1338 (m), 1193 (m), 1090 (w), 1054 (w), 988 (m), 955 (m), 915 (m), 788 (s), 663 (m), 554 (m).

2.3.2. Synthesis of $[\text{Me}_2\text{Sn}(\text{L}^1)_2]$ (**2**)

An analogous method to that used for the preparation of **1** was followed using Me_2SnCl_2 (0.10 g, 0.45 mmol) and $\text{c-C}_3\text{H}_6\text{NH}_3^+(\text{L}^1)^-$ (0.17 g, 0.90 mmol). Colorless crystals of **2** suitable for diffraction studies were obtained after several successive attempts of slow evaporation of dichloromethane solutions of the product. Yield: 0.13 g (69%). M.p.: 128-129 °C. Anal. found: C, 29.35; H, 4.09; N, 6.80. Calcd. for $\text{C}_{10}\text{H}_{18}\text{N}_2\text{S}_4\text{Sn}$: C, 29.07; H, 4.39; N, 6.78%. ^1H NMR (CDCl_3) δ_{H} (ppm): 7.62 (s, 2H, 2NH), 2.98-2.87 (m, 2H, 2CH), 1.56 (s, 6H, SnMe_2), 0.93-0.87 (m, 4H, 2 CH_2), 0.79-0.73 (m, 4H, 2 CH_2). ^{13}C NMR ($\text{CDCl}_3+\text{DMSO}-d_6$) δ_{C} (ppm): 201.06 (C=S), 29.36 (CH), 13.76 (CH_2), 5.59 ($^1J(^{13}\text{C}-^{119}\text{Sn})$ 317 Hz, SnMe_2). ^{119}Sn NMR (CDCl_3) δ_{Sn} (ppm): -273.3 . IR absorption (cm^{-1}): 3188 (s), 2997 (w), 2930 (s), 2852 (m), 1634 (m), 1520 (s), 1448 (m), 1379 (m), 1343 (m), 1252 (w), 1155 (w), 1084 (w), 988 (s), 889 (m), 789 (m), 738 (w), 644 (m), 557 (w).

2.3.3. Synthesis of $[\text{Me}_2\text{Sn}(\text{L}^2)_2]$ (**3**)

An analogous method to that used for the preparation of **1** was followed using Me_2SnCl_2 (0.10 g, 0.45 mmol) and $\text{c-C}_6\text{H}_{12}\text{NH}_3^+(\text{L}^2)^-$ (0.25 g, 0.90 mmol). Colorless crystals of **3** suitable for diffraction studies were obtained after several successive attempts of slow evaporation of dichloromethane solutions of the product. Yield: 0.15 g (66%). M.p.: 145-146 °C. Anal. found: C, 38.88; H, 6.25; N, 5.60. Calcd. for $\text{C}_{16}\text{H}_{30}\text{N}_2\text{S}_4\text{Sn}$: C, 38.64; H, 6.08; N, 5.63%. ^1H NMR

(CDCl₃) δ_H (ppm): 7.48 (s, 2H, 2NH), 3.93-3.87 (m, 2H, 2CH), 2.10-1.14 (m, 20H, 10CH₂), 0.88 (s, 6H, SnMe₂). ¹³C NMR (CDCl₃) δ_c (ppm): 204.16 (C=S), 55.29 (CH), 31.75, 24.93, 24.58 (CH₂), 4.74 (¹J(¹³C-¹¹⁹Sn) 406 Hz, SnMe₂). ¹¹⁹Sn NMR (CDCl₃) δ_{Sn} (ppm): -270.5. IR absorption (cm⁻¹): 3214 (s), 2979 (m), 2849 (w), 1636 (m), 1511 (s), 1420 (w), 1368 (m), 1334 (s), 1208 (w), 1182 (m), 1094 (w), 1027 (s), 1005 (w), 965 (m), 912 (m), 823 (w), 797 (s), 759 (w), 699 (w), 636 (m), 558 (w).

2.3.4. Synthesis of [*n*-Bu₂Sn(L²)₂] (**4**)

An analogous method to that used for the preparation of **1** was followed using *n*-Bu₂SnCl₂ (0.10 g, 0.32 mmol) and $\text{C}_6\text{H}_{12}\text{NH}_3^+(\text{L}^2)^-$ (0.18 g, 0.65 mmol). Colorless crystals of **4** suitable for diffraction studies were obtained after several successive attempts of slow evaporation of dichloromethane solutions of the product. Yield: 0.10 g (52%). M.p.: 127-128 °C. Anal. found: C, 45.86; H, 7.02; N, 5.12. Calcd. for C₂₂H₄₂N₂S₄Sn: C, 45.44; H, 7.28; N, 4.82%. ¹H NMR (CDCl₃) δ_H (ppm): 7.46 (d, ³J(¹H-¹H) 8 Hz, 2H, 2NH), 3.99-3.87 (m, 2H, 2CH), 2.15-1.55 (m, 20H, 10CH₂), 1.50-0.85 (m, 18H, Sn(*n*-Bu)₂). ¹³C NMR (CDCl₃) δ_c (ppm): 201.18 (C=S), 57.90 (CH), 34.39, 31.87, 28.40 (CH₂), 26.32, 25.18, 24.66, 13.74 (¹J(¹³C-¹¹⁹Sn) 289 Hz, Sn(*n*-Bu)₂). ¹¹⁹Sn NMR (CDCl₃) δ_{Sn} (ppm): -278.9. IR absorption (cm⁻¹): 3180 (s), 2988 (w), 2926 (s), 2853 (m), 1634 (m), 1515 (s), 1448 (m), 1378 (m), 1340 (m), 1257 (w), 1185 (w), 1151 (w), 1086 (w), 1050 (w), 1017 (w), 984 (s), 887 (m), 795 (w), 726 (w), 688 (w), 645 (m), 574 (w).

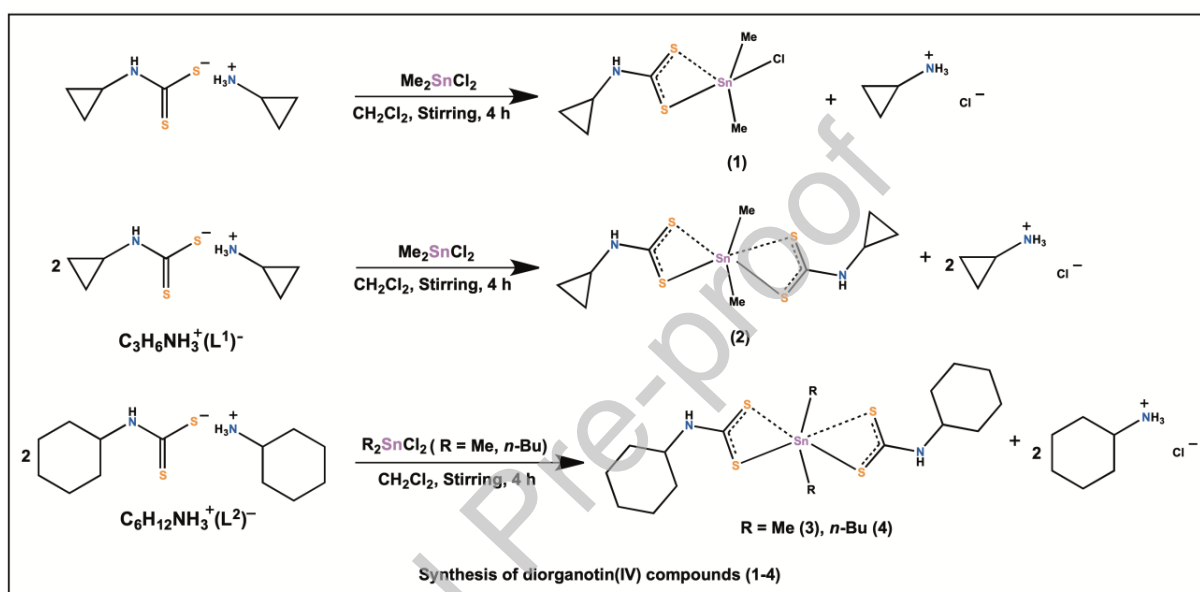
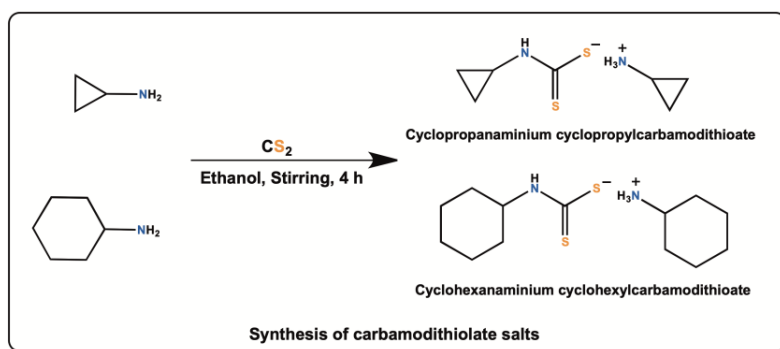
2.4. X-ray crystallography

The measurements were performed on an Agilent Technologies four-circle Gemini diffractometer [34] using Mo K α radiation ($\lambda = 0.71073 \text{ \AA}$) from a fine-focus sealed X-ray source. Full spheres of data were collected using omega scans of 0.5° per frame. Data reduction was performed with CrysAlisPro [35]. Intensities were corrected for Lorentz and polarization effects and empirical absorption corrections using spherical harmonics were applied [35]. The structures were solved by direct methods using the SIR97 package [36] and refined with SHELXL-2018/3 [37]. Calculations were performed using the WinGX System-Version 2018-3 [38]. C-bonded hydrogen atoms were included in the refinement in calculated positions using the riding model approximation with the $U_{\text{iso}}(\text{H})$ defined as $1.2U_{\text{eq}}$ and $1.5U_{\text{eq}}$ of the parent methylene and methyl atoms, respectively. Hydrogen atoms attached to N were located from the difference Fourier map and refined according to the riding model with $U_{\text{iso}}(\text{H})$ as $1.5U_{\text{eq}}$ of the parent N-atom. Least square refinements with anisotropic thermal motion parameters for all the non-hydrogen atoms were employed. Crystallographic data given in Table 1 and Table 2 present a comparison of the structural parameters of the compounds and will be recurrently referred to in the discussion of the structures (see below). Illustrative hydrogen-bond interactions are shown in the Supplementary Material file, Figs. S20-S24, and data on such non-covalent contacts are presented in Table S1.

3. Results and discussion

3.1. Synthesis and spectroscopic characterization of $\text{c-C}_3\text{H}_6\text{NH}_3^+(\text{L}^1)^-$ and $\text{c-C}_6\text{H}_{12}\text{NH}_3^+(\text{L}^2)^-$ and diorganotin(IV) compounds **1-4**

Treatment of cyclopropylamine /cyclohexylamine with carbon disulfide in 2:1 molar ratio in ethanol delivered the respective carbamodithioate salts $\text{c-C}_3\text{H}_6\text{NH}_3^+(\text{L}^1)^-$ and $\text{c-C}_6\text{H}_{12}\text{NH}_3^+(\text{L}^2)^-$ in good yields instead of the carbamodithioic acid reported earlier [26]. The diorganotin(IV) compounds were obtained via simple metathesis between the $\text{c-C}_3\text{H}_6\text{NH}_3^+(\text{L}^1)^-$ or $\text{c-C}_6\text{H}_{12}\text{NH}_3^+(\text{L}^2)^-$ salts and the diorganotin dichlorides in dichloromethane (Scheme 1). The by-products were identified through their melting points as cyclopropanaminium chloride (cyclopropylamine hydrochloride), 85-86 °C [39] and cyclohexanaminium chloride (cyclohexylamine hydrochloride), 206-209 °C [40], the latter also by SCXRD. The structural features of the carbamodithiolate salts and diorganotin(IV) compounds **1-4** were envisioned from IR, ^1H , ^{13}C (additionally by ^{119}Sn NMR for **1-4**) spectroscopic methods and by SCXRD.



Scheme 1. Systematic representation of the reaction methodology for the preparation of c - $C_3H_6NH_3^+(L^1)^-$ and c - $C_6H_{12}NH_3^+(L^2)^-$ carbamodithiolate salts and their reactions with diorganotin dichloride to afford compounds **1-4**.

All the IR spectra displayed a characteristic broad band at around 3450 cm^{-1} assigned to $\nu(\text{NH})$. A strong band due to $\nu(\text{C-N})$ was detected at 1558 and 1481 cm^{-1} for c - $C_3H_6NH_3^+(L^1)^-$ and c - $C_6H_{12}NH_3^+(L^2)^-$, respectively, while in compounds **1-4** that band was perceived in the range 1512 - 1536 cm^{-1} , coincidentally well within the region (1450 - 1550 cm^{-1}) for the NCSN thiourea group. Compounds **2-4** displayed a single strong vibration in the range 984 to 1027

cm^{-1} , suggesting a bidentate binding of the dithiocarbamate moiety; in **1** the splitting of this band corroborates an unsymmetrical binding environment [23,41]. However, bidentate bonding mode of CS_2 could not be determined on the basis of $\Delta\nu$ value [$\Delta\nu = \nu(\text{CS}_2)_{\text{asy}} - \nu(\text{CS}_2)_{\text{sy}}$] as $\nu(\text{CS}_2)_{\text{sy}}$ band could not be assigned unambiguously, which was eventually confirmed from the results of the single-crystal X-ray diffraction analysis (*vide infra*).

^1H NMR of $[\text{C}_3\text{H}_6\text{NH}_3^+(\text{L}^1)]^-$ and $[\text{C}_6\text{H}_{12}\text{NH}_3^+(\text{L}^2)]^-$ displayed the expected signals due to NH and NH_3 protons, as well as the multiplets due to CH and CH_2 proton(s). The ^{13}C NMR spectra for these salts revealed the C=S groups as well as the CH and CH_2 resonances of cyclopropyl and cyclohexyl moieties (see experimental for specific assignments). The absence of ^1H and ^{13}C NMR signals for cyclopropanaminium and cyclohexanaminium moieties in **1-4** confirmed elimination of the cationic species as their anaminium chlorides (hydrochlorides). The ^1H NMR spectra of **1-4** showed the expected signals due to NH, CH, CH_2 and $\text{SnMe}_2/\text{Sn}(n\text{-Bu})_2$ groups with adequate integration values and confirming the presence of cyclopropylcarbamdithioate and cyclohexylcarbamdithioate ligands; the corresponding carbon signals in the ^{13}C NMR were also detected. The ^{119}Sn NMR spectra in CDCl_3 solution displayed a sharp singlet at -158.4 ppm for $[\text{Me}_2\text{Sn}(\text{L}^1)\text{Cl}]$ (**1**) and in the δ range of -270.5 to -278.9 for rest of the complexes. The observed $\delta(^{119}\text{Sn})$ chemical shifts are consistent with the presence of five- (in **1**) and six-coordinate (in **2-4**) complexes in solution [42,43]. The solution NMR data could not distinguish whether the dithiolate ligands are coordinated in the mono- or bidentate mode. The structures of all the compounds were confirmed by SCXRD (see below). The $^1\text{J}(^{13}\text{C}-^{119}\text{Sn})$ NMR coupling constants were used to estimate the C-Sn-C bond angle in solution using the relationship established by Lockhart et. al [44]. For compound **1** the calculated angle of 126° is similar to solid-state values of $128.5(3)$ (Sn1) and $130.4(3)^\circ$ (Sn2) (Table 2, entry 8),

suggesting the square pyramidal structure is retained in solution. On the other hand, calculated values for compounds **2-4** of 105, 112 and 102° are significantly lower than 134.7(2), 132.4(2) and 140.2(4)°, respectively, suggesting the skewed trapezoidal bipyramid arrangement is not retained in solution. When considered together with ^{119}Sn NMR chemical shifts indicative of hexacoordination, the calculated C-Sn-C bond angles suggest a distorted octahedral arrangement for compounds **2-4** in solution.

3.2. Description of the crystal structures

The asymmetric units of $\text{c-C}_3\text{H}_6\text{NH}_3^+(\text{L}^1)^-$ and $\text{c-C}_6\text{H}_{12}\text{NH}_3^+(\text{L}^2)^-$ are displayed in Fig. 1, each one including one anaminium cation and one dithiocarbamate anion. The cyclohexyl rings in $\text{c-C}_6\text{H}_{12}\text{NH}_3^+(\text{L}^2)^-$ adopt the chair conformation. The ellipsoid plots of the diorganotin(IV) compounds **1-4** are displayed in Figs. 2-5. The asymmetric units of the diorganotin(IV) compounds **2-4** (Figs. 3-5) contain one neutral molecule with the Sn cation in skewed trapezoidal bipyramid geometry.

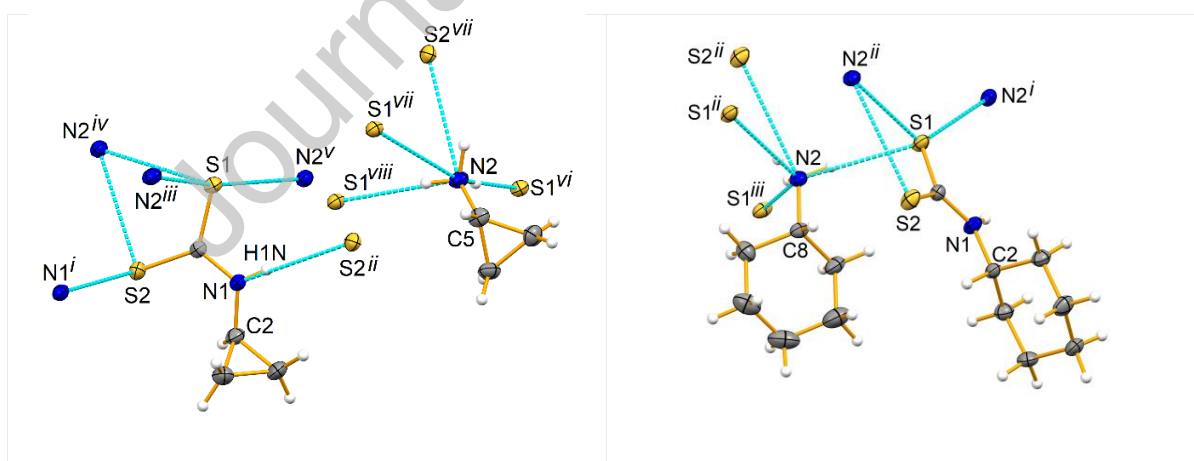


Fig. 1. Ellipsoid plots (drawn at 30% probability level) of the asymmetric units of $\text{c-C}_3\text{H}_6\text{NH}_3^+(\text{L}^1)^-$ (left) and $\text{c-C}_6\text{H}_{12}\text{NH}_3^+(\text{L}^2)^-$ (right) with partial atom labeling schemes.

Intermolecular hydrogen-bond interactions are represented as dashed light-blue lines. Symmetry operation to generated equivalent atoms: in $\text{c-C}_3\text{H}_6\text{NH}_3^+(\text{L}^1)^-$, i) $x, 1/2-y, 1/2+z$; ii) $x, 1/2-y, -1/2+z$; iii) $x, 1.5-y, 1/2+z$; iv) $x, 1.5-y, -1/2+z$; v) $x, 1+y, 1+z$; vi) $x, -1+y, -1+z$; vii) $-x, 1/2+y, 1/2-z$; viii) $-x, -1/2+y, 1/2-z$. In $\text{c-C}_6\text{H}_{12}\text{NH}_3^+(\text{L}^2)^-$, i) $-x, 1/2+y, 1/2-z$; ii) $-x, 1-y, 1-z$; iii) $-x, -1/2+y, 1/2-z$.

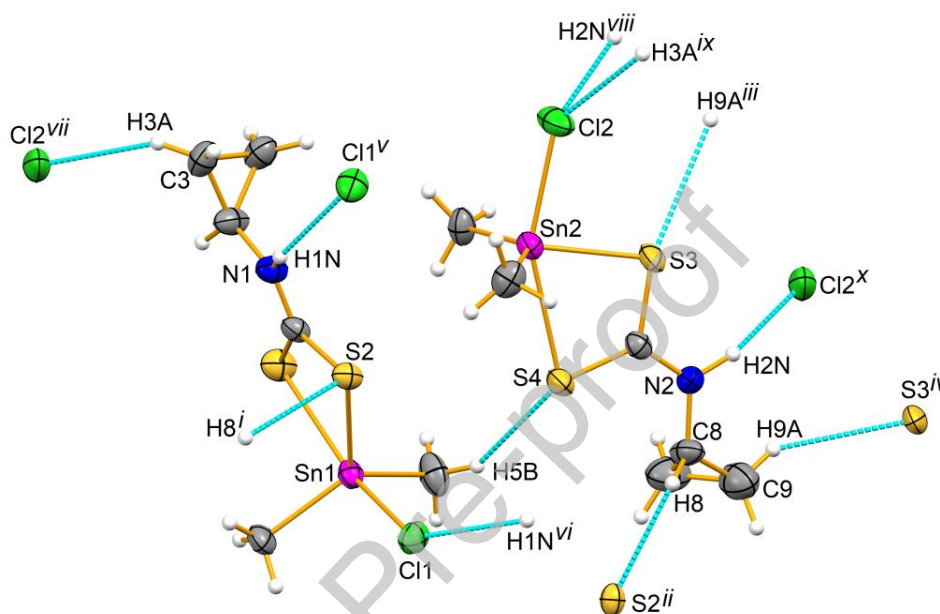


Fig. 2. Ellipsoid plot (drawn at 30% probability level) of the asymmetric unit of **1** with partial atom labeling scheme. Intermolecular hydrogen-bond interactions are represented as dashed light-blue lines. Symmetry operation to generated equivalent atoms: i) $1/2-x, -1/2+y, 1.5-z$; ii) $1/2-x, 1/2+y, 1.5-z$; iii) $1.5-x, -1/2+y, 1.5-z$; iv) $1.5-x, 1/2+y, 1.5-z$; v) $1/2-x, -1/2+y, 1.5-z$; vi) $1/2-x, 1/2+y, 1.5-z$; vii) $-1/2+x, -1/2-y, 1/2+z$; viii) $1/2+x, -1/2-y, -1/2+z$; ix) $1.5-x, -1/2+y, 1.5-z$; x) $1.5-x, -1/2+y, 1.5-z$.

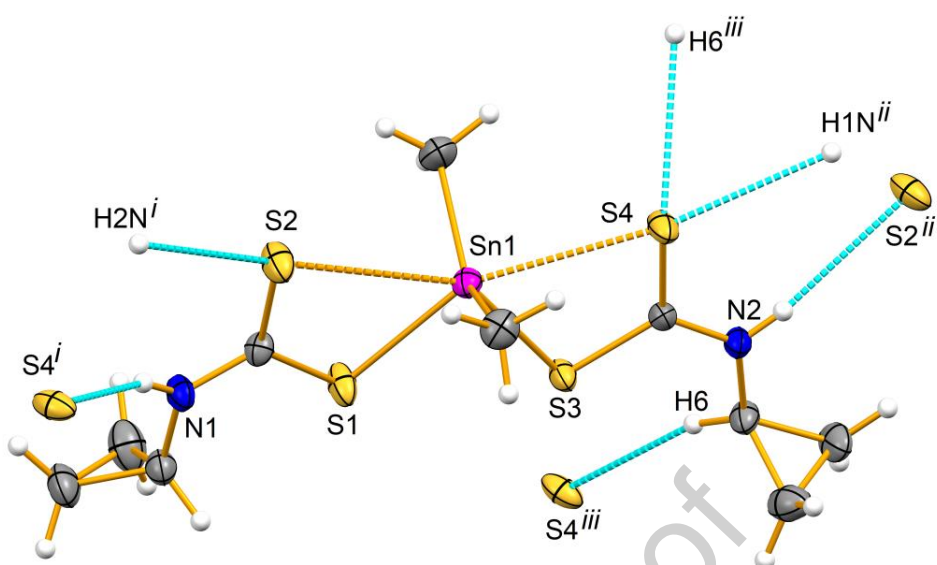


Fig. 3. Ellipsoid plot (drawn at 30% probability level) of the asymmetric unit of **2** with partial atom labeling scheme. Intermolecular hydrogen-bond interactions are represented as dashed light-blue lines. Symmetry operation to generated equivalent atoms: i) $1/2-x, -y, -1/2+z$; ii) $1/2-x, -y, 1/2+z$; iii) $1/2-x, -1/2+y, z$.

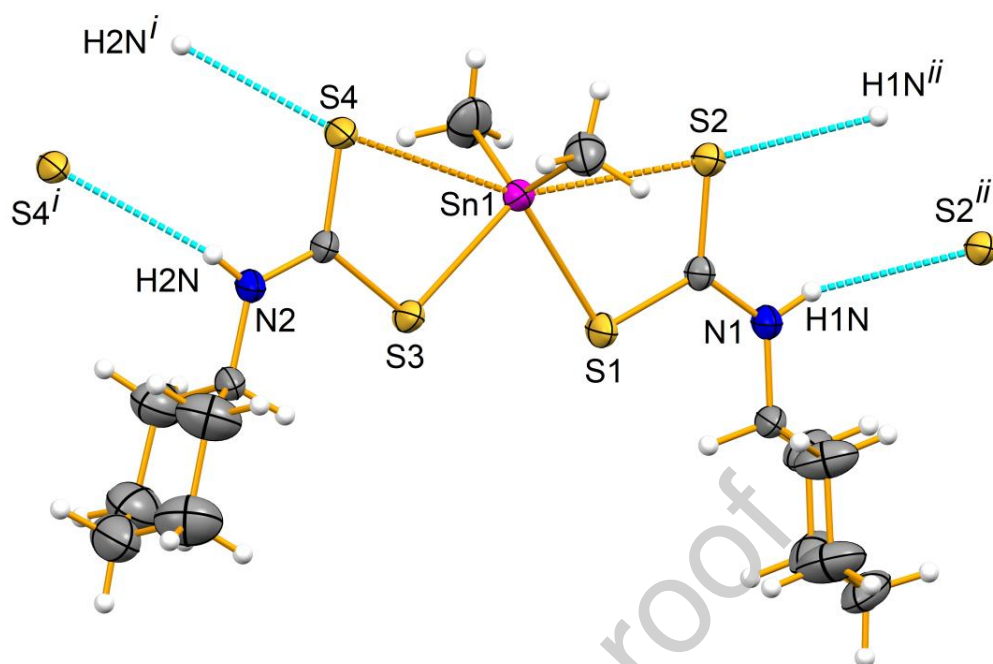


Fig. 4. Ellipsoid plot (drawn at 30% probability level) of the asymmetric unit of **3** with partial atom labelling scheme. Intermolecular hydrogen-bond interactions are represented as dashed light-blue lines. Symmetry operation to generated equivalent atoms: i) $1-x, 1-y, 1-z$; ii) $2-x, -y, 1-z$.

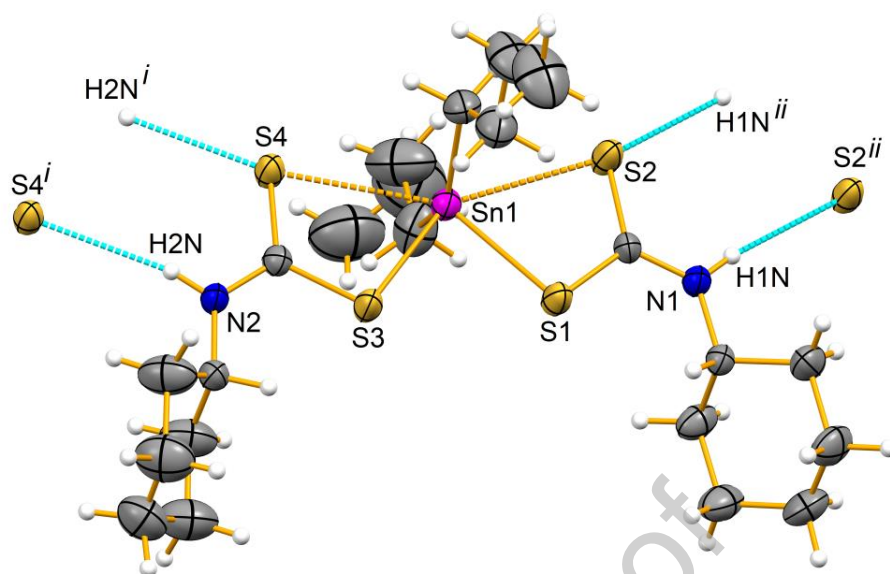


Fig. 5. Ellipsoid plot (drawn at 30% probability level) of the asymmetric unit of **4** with partial atom labeling scheme. Intermolecular hydrogen-bond interactions are represented as dashed light-blue lines. Symmetry operation to generated equivalent atoms: i) $1-x, 1-y, 1-z$; ii) $1-x, 2-y, 2-z$.

The coordination positions include two alkyl and two bidentate dithiocarbamate ligands. In each compound one of the S...Sn distance is longer (between 2.993(1) and 3.114(1) Å, Table 2 entry 5) than the other (between 2.4778(11) and 2.5167(10) Å, Table 2 entry 4) but is still shorter than the sum of the van der Waals radii of the corresponding atoms (1.89 Å for sulfur and 2.42 Å for tin) [45]. The Sn-C distances and C-Sn-C angles (entries 3 and 8) are in the range of those found in the literature. The S-C-S angles (entry 7) are generally slightly smaller than those in *c*-C₃H₆NH₃⁺(L¹)⁻ and *c*-C₆H₁₂NH₃⁺(L²)⁻. The S-Sn...S angles (denoted as *intra-ligand* S-Sn-S angles, Table 2 entry 9) vary from 63.14(3) to 64.97(3)°. The S-Sn-S angles, either involving the short [between 80.48(3)-82.96(3)°] or the long Sn-S distances [between 148.69(3)-152.77(3)°; Table 2, entry 10], fall in the range already reported, enabling classifying **2-4** in the series of compounds with structural Motif I [8]. The stereochemical effect of the *N*-substituent of the dithiocarbamate as well as of the alkyl ligands is clearly revealed by the angle between the least-square planes of the NCS₂ groups (entry 12). For example, comparing the dimethyltin(IV) complexes **2** and **3** the bulky cyclohexyl substituents in the latter decreases that angle (entry 12) to 1.86 ° (in **3**) as compared to that in the former (9.63° in **2**). This conceivably results in a compression of the crystal packing in **3** as revealed by the decrease of the shortest intermolecular Sn...Sn distance (entry 14). In contrast, when examining the cyclohexyl dithiocarbamate complexes **3** and **4**, the *n*-butyl groups in the latter impose a relative turning of the NCS₂ groups increasing the referred bite angle from 1.86 to 12.87° (entry 12) as well as the Sn...Sn distance (entry 14).

The asymmetric unit of **1** contains two neutral Sn(IV) complex molecules each displaying a square pyramidal geometry (entry 1, τ_5 of 0.43) [46] with a chelating dithiocarbamate and a chloride ligand occupying the equatorial plane and the alkyl moieties the axial site. A noticeable effect of the chloride anion is a shortening of the Sn-S lengths (in the 2.4518(14) - 2.7751(17) Å range,

entry 4) as well as the S-C-S and the C-Sn-C angles (entries 7 and 8, respectively), in comparison to what was obtained in the other complexes (see above and Table 2). The Sn-C distances (entry 3) are in the range of the ones in **2-4**. A broader range of C-Sn-S angles was measured in **1** (entry 11).

The considerably shorter intermolecular Sn...Sn distance in **1**, as compared to the other compounds (entry 14), can be related to the van der Waals S...Cl contacts (entry 13). Evaluating the cohesion force in **1** through the estimation of the contact parameter δ (eq. 1, where d_{AB} is the contact distance between atoms A and B, and vdW_A and vdW_B the respective van der Waals radii) [47], the obtained values of +0.44 Å for the S...Cl interaction (also, +0.52 Å for the S...S and +0.69 Å for the Cl...Cl ones) classifies it as very weak and irrelevant for the packing of the molecules in the crystal.

$$\delta = d_{AB} - vdW_A - vdW_B \quad (1)$$

Sets of tentative hydrogen-bond interactions (Table S1) could be detected in compounds **1-4** (Figs. S20-S23) with relevance for the N-H...S (or Cl, in **1**), as well as in $c\text{-C}_3\text{H}_6\text{NH}_3^+(\text{L}^1)^-$ and $c\text{-C}_6\text{H}_{12}\text{NH}_3^+(\text{L}^2)^-$. Such interactions make infinite 1D chains in all cases, but in **2** there is the possibility of expansion to the second dimension resulting from CH...S contacts. Indeed, for all the tin(IV) compounds the δ parameter for the N-H...S between -0.38 and -0.55 [47] (Table S1) are reasonably strong (the negative values for the δ parameter are indicative of overlapping of the van der Waals spheres) [48] and stresses the role of such contacts in extending the structure to higher dimension. The higher δ values for the ammonium dithiocarbamate salts [-0.79 Å in $c\text{-C}_3\text{H}_6\text{NH}_3^+(\text{L}^1)^-$ and -0.76 Å in $c\text{-C}_6\text{H}_{12}\text{NH}_3^+(\text{L}^2)^-$] reveals a tighter packing structure in these cases, conceivably due to the absence of coordination to a metal cation.

The 3D Hirshfeld surfaces and 2D fingerprint plots were used to further investigate the interactions between molecules of each of the compounds, the latter being a useful method for the quantification of the different interactions [49-51]. The plots over d_{norm} (Fig. 6 and Fig. S24) were obtained with the CrystalExplore software, version 17.5 [50], and consider the distances to the surface from nuclei outside (d_e) and inside (d_i) the Hirshfeld surface. These surfaces were drawn in transparent mode to visualize the molecules that gave rise to them: the red color indicates the stronger intermolecular contacts, the white those around the van der Waals radii range, and the blue the weaker contacts. In every structure the predominance of the S...H (or the Cl...H in **1**) interactions over the C...H and the N...H contacts is shown by the vivid red areas on the Hirshfeld surfaces.

The fingerprint plots of the pro-ligands and compounds **1-4** have identical overall shapes (Fig. 7). A comparison of the percentages of contribution to the total of each Hirshfeld surface is presented in Fig. 8. It can be ascertained that in every case the major contribution is from H...H contacts. These are followed by the S...H (the Cl...H interaction of 22.1 % in **1** also plays a significant role in the respective total surface), and then the C...H and the N...H contacts with a much lower influence. Since $c\text{-C}_3\text{H}_6\text{NH}_3^+(\text{L}^1)^-$, $c\text{-C}_6\text{H}_{12}\text{NH}_3^+(\text{L}^2)^-$ and **1** comprise two entities (ions or molecular units) in the structure, it is expected [52] that each component would have a different contribution to the overall Hirshfeld surfaces as shown also in Fig. 8. Indeed, in compound **1** the Sn2 molecule has a slightly higher contribution to the S...H and Cl...H intermolecular contacts than the Sn1 molecule (Fig. 8, middle). Concerning the dithiocarbamate salts (Fig. 8, bottom), the anions are the largest contributors to the S...H interactions, while the cations are for the H...H contacts.

Only in compound **2** is the shortest $d_e + d_i$ distance of the H...H type (*ca.* 2.0 Å); in the remaining cases the shortest H...H and S...H contacts have identical values (between *ca.* 2.2 and 2.5 Å), while for the Cl...H (in **1**) the shortest value reaches *ca.* 2.7 Å. Other intermolecular contacts not referred to above contribute less than 1% of the total volume of the Hirshfeld surfaces.

Journal Pre-proof

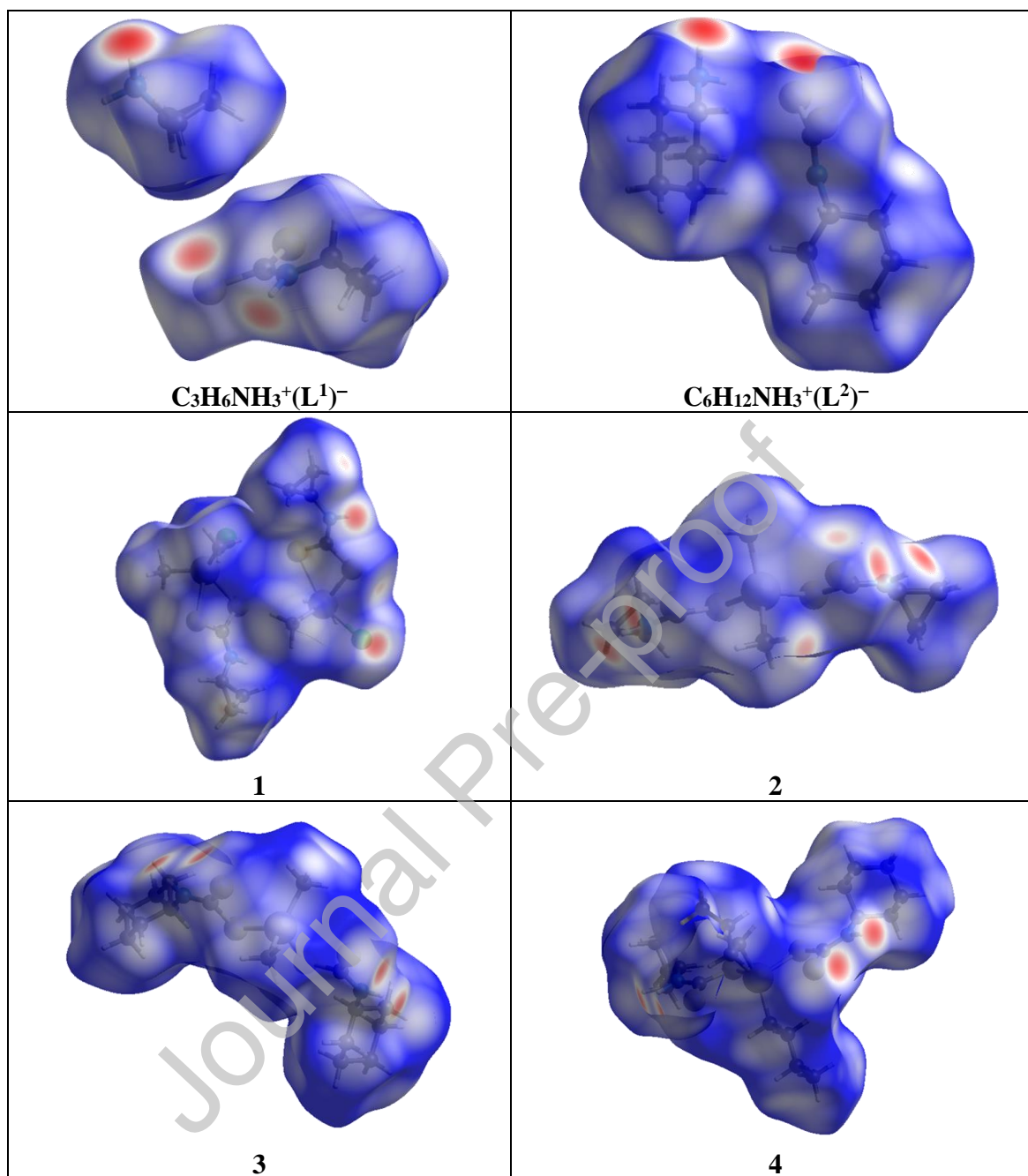


Fig. 6. Depiction of the d_{norm} Hirshfeld surfaces of the compounds in transparent mode.

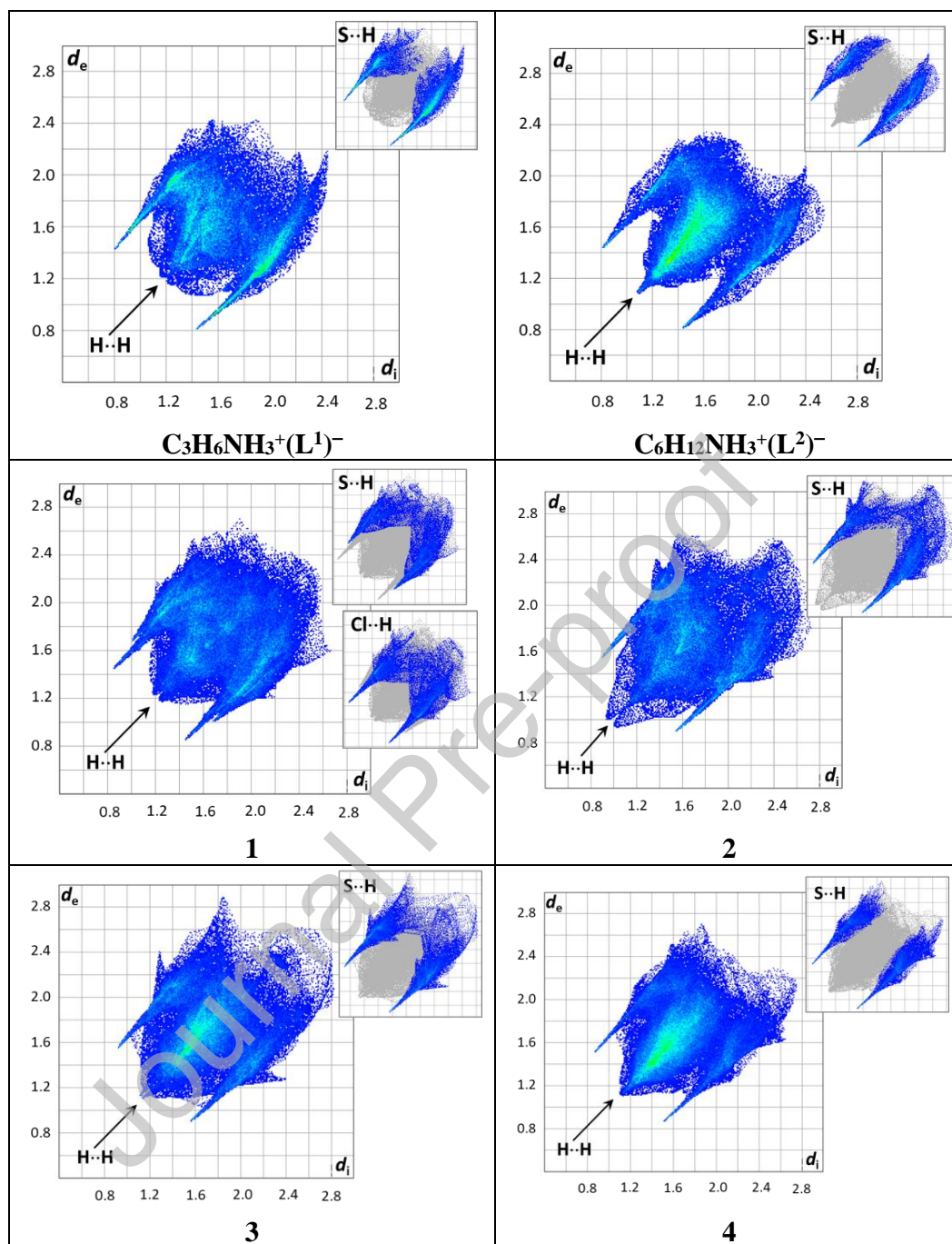


Fig. 7. Fingerprint plots for the compounds with offset representations of the $S \cdots H$ contributions (also $Cl \cdots H$ for **1**) to the total Hirshfeld surfaces.

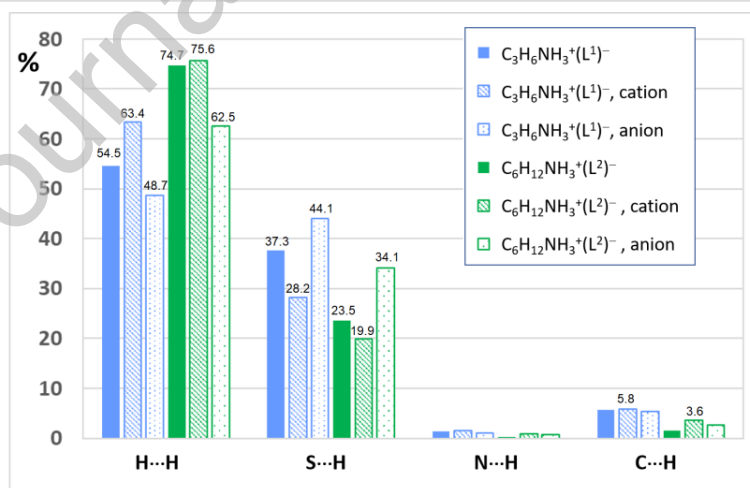
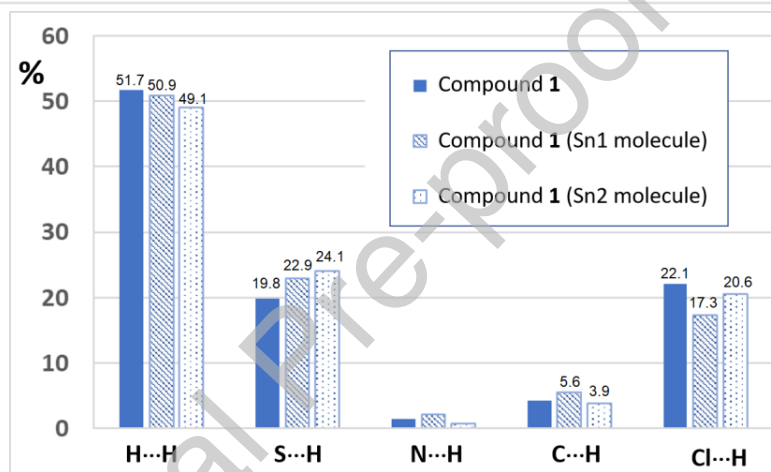
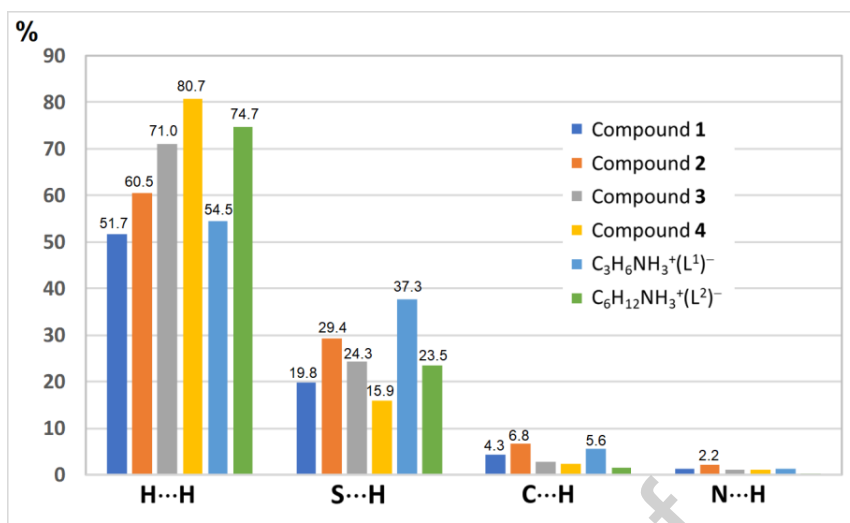


Fig. 8. Percentage contribution to the total Hirshfeld surface of the interactions in every compound (top), individual contributions of the molecules in **1** (middle), and of each ion in the dithiocarbamate salts (bottom).

4. Conclusion

An efficient and highly practical method for the synthesis of **new** diorganotin(IV) dithiocarbamates is described. Cyclopropanaminium cyclopropylcarbamodithioate and cyclohexanaminium cyclohexylcarbamodithioate salts produced **new** diorganotin(IV) dithiocarbamates upon reactions with diorganotin dihalide by metathesis. The method can be considered as environmentally friendly since sodium/potassium/ammonium hydroxides, commonly used in the preparation of Na/K/NH₄-dithiocarbamates, were avoided. The advantages of the described protocol are due to the synthetic simplicity, high to excellent yield of products, and the ability of the obtained carbamodithioate salts to react with organometal compounds in one step. The H···H intermolecular contacts are the main contributors to the total volume of the Hirshfeld surfaces, followed by the S···H interactions. In cases where there are more than one component in the crystal (as in the structures of **1** and of the dithiocarbamate salts) the individual entities contribute in slightly different extents to the overall Hirshfeld surface.

Conflict of interest

The authors declare that they have no conflicts of interest with the contents of this article.

Acknowledgements

Financial support from the Department of Biotechnology, India (Grant No. BT/PR25263/NER/95/1104/2017, TSBB) and Fundação para a Ciência e a Tecnologia (FCT), Portugal, (projects UID/QUI/00100/2019 and multiannual funding 2020-2023 to Centro de Química Estrutural, MFCGS) are gratefully acknowledged. MRA thanks University Grants Commission for the award of non-NET and UGC-JRF fellowships. TSBB and MRA acknowledge access to DST-PURSE for the diffractometer facility.

Appendix A. Supplementary data

CCDC-2013890-2013895 contains the supplementary crystallographic data for the compounds reported in this paper: $\text{c-C}_3\text{H}_6\text{NH}_3^+(\text{L}^1)^-$ (2013892), $\text{c-C}_6\text{H}_{12}\text{NH}_3^+(\text{L}^2)^-$ (2013894) and **1** (2013890), **2** (2013895), **3** (2013891) and **4** (2013893). These data can be obtained free of charge via <http://www.ccdc.cam.ac.uk/conts/retrieving.html>, or from the Cambridge Crystallographic Data Center, 12 Union Road, Cambridge CB2 1EZ, UK; fax: (+44) 1223-336-033; or e-mail: deposit@ccdc.cam.ac.uk.

IR spectra (Figs. S1-S6), ^1H , ^{13}C , and ^{119}Sn NMR spectra (Figs. S7-S19), X-ray: H-bonding interactions (Figs. S20-S23), Hirshfeld surfaces (Fig. S24), structural parameters involving H-bond interactions in $\text{c-C}_3\text{H}_6\text{NH}_3^+(\text{L}^1)^-$, $\text{c-C}_6\text{H}_{12}\text{NH}_3^+(\text{L}^2)^-$ and **1-4** (Table S1).

CREDIT AUTHOR STATEMENT

T. S. Basu Baul: Conceptualization, Methodology, Supervision, Project administration, Funding acquisition, Writing - Review & Editing. **Maheswara Rao Addepalli:** Investigation, Methodology, Data curation. **Andrew Duthie:** Investigation, Visualization, Writing - Review &

Editing. M. Fátima C. Guedes da Silva: Analysis, Validation, Review & Editing, Funding acquisition.

References

- [1] A. Z. Halimehjani, Y. L. Nosood, *Org. Lett.* 19 (2017) 6748-6751 and reference therein.
- [2] M. Marinovich, B. Viviani, V. Capra, E. Corsini, L. Anselmi, G. D'Agostino, A. D. Nucci, M. Binaglia, M. Tonini, C. L. Galli, *Chem. Res. Toxicol.* 15 (2002) 26-32.
- [3] P. J. Nieuwenhuizen, A. W. Ehlers, J. G. Haasnoot, S. R. Janse, J. Reedijk, E. J. Baerends, *J. Am. Chem. Soc.* 121 (1999) 163-168.
- [4] (a) J. T. Lai, R. J. Shea, *Polym. Sci. Part A: Polym. Chem.* 44 (2006) 4298-4316. (b) A. Duréault, Y. Gnanou, D. Taton, M. Destarac, F. Leising, *Angew. Chem., Int. Ed.* 42 (2003) 2869-2872.
- [5] (a) A. Z. Halimehjani, Y. Pourshojaei, M. R. Saidi, *Tetrahedron Lett.* 50 (2009) 32-34 (b) O. Rozen, E. Mishani, S. Rozen, *Tetrahedron* 66 (2010) 3579-3582.
- [6] X. L. Hou, Z. M. Ge, T. M. Wang, W. Guo, J. R. Cui, T. M. Cheng, C. S. Lai, R. T. Li, *Bioorg. Med. Chem. Lett.* 16 (2006) 4214-4219.
- [7] S. Tamilvanan, G. Gurumoorthy, S. Thirumaran, S. Ciattini, 121 (2017) 70-79.
- [8] E. R. T. Tiekink, *Appl. Organomet. Chem.* 22 (2008) 533-550.
- [9] J. O. Adeyemi, D. C. Onwudiwe, M. Singh, *J. Mol. Struct.* 1179 (2019) 366-375.
- [10] A. G. Davies, M. Gielen, K. Pannel, E. R. T. Tiekink (Eds.), *Tin Chemistry: Fundamentals and Frontiers*, Wiley, Chichester, 2008.
- [11] K. Ramasamy, V. L. Kuznetsov, K. Gopal, M. A. Malik, J. Raftery, P. P. Edwards, P. O'Brien, *Chem. Mater.* 25 (2013) 266-276.
- [12] P. Selvaganapathi, S. Thirumaran, S. Ciattini, *Appl. Organomet. Chem.* (2019) e5089.

- [13] A. N. Gupta, V. Kumar, V. Singh, A. Rajput, L. B. Prasad, M. G. B. Drew, N. Singh, J. Organomet. Chem. 787 (2015) 65-72.
- [14] J. P. Fuentes-Martínez, I. Toledo-Martínez, P. Román-Bravo, P. G. García, C. Godoy-Alcántar, M. López-Cardoso, H. Morales-Rojas, Polyhedron 28 (2009) 3953-3966.
- [15] J. Cruz-Huerta, M. Carillo-Morales, E. Santacruz-Juárez, I. F. Hernández-Ahuactzi, J. Escalante-García, C. Godoy-Alcantar, J. A. Guerrero-Alvarez, H. Höpfl, H. Morales-Rojas, M. Sánchez, Inorg. Chem. 47 (2008) 9874-9885.
- [16] M. G. Vasquez-Ríos, V. Reyes- Márquez, H. Höpfl, A. Torres-Huerta, J. Guerrero-Álvarez, M. Sánchez, I. F. Hernández-Ahuactzi, K. Ochoa-Lara, A. Jiménez-Sánchez, R. Santillán, Eur. J. Inorg. Chem. (2016) 3429-3440.
- [17] J. Cookson, P. D. Beer, Dalton Trans. (2007) 1459-1472.
- [18] E. Santacruz-Juárez, J. Cruz-Huerta, I. F. Hernández-Ahuactzi, R. Reyes-Martinez, H. Tlahuext, H. Morales-Rojas, H. Höpfl, Inorg. Chem. 47 (2008) 9804-9812.
- [19] I. Rojas-León, H. Alnasr, K. Jurkschat, M. G. Vasquez-Ríos, G. Gómez-Jaimes, H. Höpfl, I. F. Hernández-Ahuactzi, R. Santillan, Organometallics 38 (2019) 2443-2460.
- [20] M. Nath, S. Pokharia, R. Yadav, Coord. Chem. Rev. 215 (2001) 99-149.
- [21] L. Nagy, A. Szorcsik, K. Kovács, Acta Pharm. Hung. 70 (2000) 53-71.
- [22] J. O. Adeyemi, D. C. Onwudiwe, A. C. Ekennia, R. C. Uwaoma, E. C. Hosten, Inorg. Chim. Acta 477 (2018) 148-159.
- [23] J. O. Adeyemi, D. C. Onwudiwe, Molecules 23 (2018) 2571; doi:10.3390/molecules23102571.
- [24] J. W. D. F. Oliveira, H. A. O. Rocha, W. M. T. Q. D. Medeiros, M. S. Silva, Molecules 24 (2019) 2806; doi:10.3390/molecules24152806.

- [25] A. T. Odularu, P. A. Ajibade, *Bioinorg. Chem. Appl.* (2019) Article ID 8260496, doi.org/10.1155/2019/8260496.
- [26] S. Jabbar, I. Shahzadi, R. Rehmany, H. Iqbal, Qurat-UI-Ain, A. Jamil, R. Kousar, S. Ali, S. Shahzadi, M. A. Choudhary, M. Shahid, Q. M. Khan, S. K. Sharma, K. Qanungo, *J. Coord. Chem.* 65 (2012) 572-590.
- [27] O.-S. Jung, Y. S. Sohn, J. A. Ibers, *Inorg. Chem.* 25 (1986) 2273-2275.
- [28] G. Hogarth, *Transition Metal Dithiocarbamates: 1978-2003*, in *Progress in Inorganic Chemistry*; K. D. Karlin (Eds.), John Wiley, London, UK, 2005, Volume 53, pp. 71-561.
- [29] S. Kanchi, P. Singh, K. Bisetty, *Arab. J. Chem.* 7 (2014) 11-25.
- [30] W. Hanefeld, G. Glaeske, P. Schulze-Weisschu, *Arch. Pharm.* 314 (1981) 587-594.
- [31] E. A. Tarakhtii, L. P. Sidorova, O. A. Zhigal'skii, O. N. Chupakhin, *Pharm. Chem. J.* 32 (1998) 15-19.
- [32] W. Fathalla, I. A. I. Ali, P. Pazdera, *Beilstein J. Org. Chem.* 13 (2017) 174-181.
- [33] M. I. Megahed, W. Fathalla, *J. Heterocyclic Chem.* 55 (2018) 2809-2816.
- [34] Agilent Technologies, XRD Products, Yarnton, Oxfordshire, England.
- [35] CrysAlisPRO, Oxford Diffraction /Agilent Technologies UK Ltd, Yarnton, England.
- [36] A. Altomare, M. C. Burla, M. Camalli, G. Cascarano, C. Giacovazzo, A. Guagliardi, A. G. Moliterni, G. Polidori, R. Spagna, *J. Appl. Crystallogr.* 32 (1999) 115-119.
- [37] G. M. Sheldrick, *Acta Crystallogr.* C71 (2015) 3-8.
- [38] L. J. Farrugia, *J. Appl. Crystallogr.* 45 (2012) 849-854.
- [39] G. D. Jones, *J. Org. Chem.* 9 (1944) 484-499.
- [40] H. W. Smith, D. Mastropaolo, A. Camerman, N. Camerman, *J. Chem. Crystallogr.* 24 (1994) 239-242.

- [41] F. Bonati, R. Ugo, *J. Organomet. Chem.* 10 (1967) 257-268.
- [42] J. Otera, *J. Organomet. Chem.* 221 (1981) 57-61.
- [43] D. Dakternieks, H. Zhu, D. Masi, C. Mealli, *Inorg. Chem.* 31 (1992) 3601-3606.
- [44] T. P. Lockhart, W. F. Manders, J. J. Zuckemann, *J. Am. Chem. Soc.* 107 (1985) 4546-4547.
- [45] S. Alvarez, *Dalton Trans.* 42 (2013) 8617-8636.
- [46] A. W. Addison, T. N. Rao, J. Reedijk, J. van Rijn, G. C. Verschoor, *J. Chem. Soc. Dalton Trans.* (1984) 1349-1356.
- [47] M. Kaźmierczak, A. Katrusiak, *CrystEngComm* 17 (2015) 9423-9430.
- [48] M. Kaźmierczak, A. Katrusiak, *Acta Crystallogr. B* 75 (2019) 865-869.
- [49] M. A. Spackman, J. J. McKinnon, *CrystEngComm* 4 (2002) 378-392.
- [50] M. A. Spackman, D. Jayatilaka, *CrystEngComm* 11 (2009) 19-32.
- [51] H. F. Clausen, M. S. Chevallier, M. A. Spackman, B. B. Iversen, *New J. Chem.* 34 (2010) 193-199.
- [52] S. L. Tan, M. M. Jotani, E. R. T. Tiekink, *Acta Cryst.* E75 (2019) 308-318.

Table 1. Crystal data and structure refinement details for $\text{c-C}_3\text{H}_6\text{NH}_3^+(\text{L}^1)^-$, $\text{c-C}_6\text{H}_{12}\text{NH}_3^+(\text{L}^2)^-$ and compounds **1–4**.

	$\text{c-C}_3\text{H}_6\text{NH}_3^+(\text{L}^1)^-$	$\text{c-C}_6\text{H}_{12}\text{NH}_3^+(\text{L}^2)^-$	1	2	3	4
Empirical formula	$\text{C}_7\text{H}_{14}\text{N}_2\text{S}_2$	$\text{C}_{13}\text{H}_{26}\text{N}_2\text{S}_2$	$\text{C}_6\text{H}_{12}\text{ClNS}_2\text{Sn}$	$\text{C}_{10}\text{H}_{18}\text{N}_2\text{S}_4\text{Sn}$	$\text{C}_{16}\text{H}_{30}\text{N}_2\text{S}_4\text{Sn}$	$\text{C}_{22}\text{H}_{42}\text{N}_2\text{S}_4\text{Sn}$
Formula weight	190.32	274.48	316.43	413.19	497.35	581.50
Crystal system	monoclinic	monoclinic	monoclinic	orthorhombic	monoclinic	triclinic
Space group	$P2_1/c$	$P2_1/c$	$P2_1/n$	$Pbca$	$P2_1/c$	$P\bar{1}$
a (Å)	12.1027(8)	14.5626(8)	13.2400(12)	13.4097(11)	17.5885(11)	11.6671(6)
b (Å)	8.4518(6)	9.7567(8)	12.4113(11)	12.7686(8)	10.6999(8)	11.9762(8)
c (Å)	9.9822(7)	11.0756(7)	14.2291(11)	19.4835(13)	12.3594(8)	12.3199(7)
α (°)	90	90	90	90	90	66.906(6)
β (°)	105.377(8)	100.775(6)	90.422(8)	90	95.795(5)	88.979(5)
γ (°)	90	90	90	90	90	66.616(6)
V (Å ³)	984.52(12)	1545.91(18)	2338.1(3)	3336.0(4)	2314.1(3)	1433.92(17)
Z	4	4	8	8	4	2
D_{calc} (g/cm ³)	1.284	1.179	1.798	1.645	1.428	1.347
$F(000)$	408	600	1232	1648	1016	604
μ (mm ⁻¹)	0.484	0.922	2.719	2.015	1.466	1.193
Reflections measured	3595	6089	6674	8414	9297	9892
Obs. / Unique reflections	2232 / 1897	3501 / 2666	4618 / 3498	3855 / 2929	5339 / 3954	6501 / 4751
No. of parameters	112	166	209	160	216	268
R_{int}	0.0201	0.0284	0.0230	0.0272	0.0300	0.0290
$R(F)$ ($I \geq 2\sigma$)	0.0367	0.0528	0.0430	0.0417	0.0491	0.0615
$wR(F^2)$ (all data)	0.0924	0.1195	0.0905	0.0837	0.1030	0.1606
GOF (F^2)	1.068	1.134	1.079	1.065	1.188	1.053
max., min. $\Delta\rho$ (e/Å ³)	0.205, -0.214	0.339, -0.248	0.682, -0.628	0.545, -0.499	0.648, -0.513	0.925, -0.594

Table 2Selected bond lengths (Å) and intramolecular distances (Å) for diorganotin(IV) compounds **1-4**.

Entry		1	2	3	4
1	Metal geometry	Square pyramid ($\tau_5 = 0.43$)	Skew trapezoidal bipyramid	Skew trapezoidal bipyramid	Skew trapezoidal bipyramid
2	C _{dithiocarboxylate} -N ^a	1.320(7) (<i>Sn2</i>) 1.299(7) (<i>Sn1</i>) 2.118(5) (<i>Sn1</i>)	1.326(5) 1.319(4)	1.323(5) 1.302(5)	1.316(6) 1.313(6)
3	Sn-C	2.109(6) (<i>Sn1</i>) 2.108(6) (<i>Sn2</i>) 2.108(5) (<i>Sn2</i>)	2.123(4) 2.118(4)	2.114(4) 2.094(5)	2.156(9) 2.131(6)
4	Sn-S	2.7170(18) (<i>Sn1</i>) 2.4518(14) (<i>Sn1</i>) 2.7751(17) (<i>Sn2</i>) 2.4625(16) (<i>Sn2</i>)	2.5167(10) 2.5057(10)	2.5049(11) 2.4778(11)	2.5047(15) 2.4991(15)
5	Sn...S	-	3.114(1) 2.993(1)	3.095(1) 3.067(1)	3.059(3) 3.049(3)
6	Sn-Cl	2.5190(15) (<i>Sn1</i>) 2.4808(17) (<i>Sn2</i>)	-	-	-
7	S-C-S ^b	118.9(3) (<i>Sn1</i>) 119.2(3) (<i>Sn2</i>)	120.7(2) 122.0(2)	120.2(2) 121.2(2)	120.6(3) 120.7(3)
8	C-Sn-C	128.5(3) (<i>Sn1</i>) 130.4(3) (<i>Sn2</i>)	134.70(19)	132.4(2)	140.2(4)
9	Intra-ligand S-Sn-S	69.68(5) (<i>Sn1</i>) 68.40(5) (<i>Sn2</i>)	63.37(3) 64.97(3)	63.14(3) 63.69(4)	63.73(6) 63.84(6)
10	S _{short} -Sn-S _{short} S _{long} -Sn-S _{long}	-	82.96(3) 148.69(3)	80.48(3) 152.77(3)	82.59(5) 149.82(6)
11	C-Sn-S	93.18(17) <i>to</i> 115.45(18)	104.48(14) <i>to</i> 109.80(14)	106.40(17) <i>to</i> 108.86(16)	102.7(3) <i>to</i> 106.8(2)
12	∠ l.s planes of the dithiocarbamate groups	-	9.63	1.86	12.87
13	Shortest intermolecular S...S (or Cl) ^c	4.122(2) for S...S, 3.987(3) for S...Cl	4.034(1)	4.020(2)	4.291
14	Shortest Sn...Sn	5.629	6.408	6.189	6.506

^a For **1**-C₃H₆NH₃⁺(L¹)⁻ and **2**-C₆H₁₂NH₃⁺(L²)⁻, 1.332(2) and 1.334(3) Å, respectively.^b For **1**-C₃H₆NH₃⁺(L¹)⁻ and **2**-C₆H₁₂NH₃⁺(L²)⁻, 123.7(1) and 122.0(1)°, respectively.^c For **1**-C₃H₆NH₃⁺(L¹)⁻ and **2**-C₆H₁₂NH₃⁺(L²)⁻, S...S of 3.9588(6) and 4.7564(9) Å, respectively.

Legends to Scheme and Figs.

Scheme 1. Systematic representation of the reaction methodology for the preparation of **c**-C₃H₆NH₃⁺(L¹)⁻ and **c**-C₆H₁₂NH₃⁺(L²)⁻ carbamodithiolate salts and their reactions with diorganotin dichloride to afford compounds **1-4**.

Fig. 1. Ellipsoid plots (drawn at 30% probability level) of the asymmetric units of **c**-C₃H₆NH₃⁺(L¹)⁻ (left) and **c**-C₆H₁₂NH₃⁺(L²)⁻ (right) with partial atom labeling schemes. Intermolecular hydrogen-bond interactions are represented as dashed light-blue lines. Symmetry operation to generated equivalent atoms: in **c**-C₃H₆NH₃⁺(L¹)⁻, i) $x, 1/2-y, 1/2+z$; ii) $x, 1/2-y, -1/2+z$; iii) $x, 1.5-y, 1/2+z$; iv) $x, 1.5-y, -1/2+z$; v) $x, 1+y, 1+z$; vi) $x, -1+y, -1+z$; vii) $-x, 1/2+y, 1/2-z$; viii) $-x, -1/2+y, 1/2-z$. In **c**-C₆H₁₂NH₃⁺(L²)⁻, i) $-x, 1/2+y, 1/2-z$; ii) $-x, 1-y, 1-z$; iii) $-x, -1/2+y, 1/2-z$.

Fig. 2. Ellipsoid plot (drawn at 30% probability level) of the asymmetric unit of **1** with partial atom labeling scheme. Intermolecular hydrogen-bond interactions are represented as dashed light-blue lines. Symmetry operation to generated equivalent atoms: i) $1/2-x, -1/2+y, 1.5-z$; ii) $1/2-x, 1/2+y, 1.5-z$; iii) $1.5-x, -1/2+y, 1.5-z$; iv) $1.5-x, 1/2+y, 1.5-z$; v) $1/2-x, -1/2+y, 1.5-z$; vi) $1/2-x, 1/2+y, 1.5-z$; vii) $-1/2+x, -1/2-y, 1/2+z$; viii) $1/2+x, -1/2-y, -1/2+z$; ix) $1.5-x, -1/2+y, 1.5-z$; x) $1.5-x, -1/2+y, 1.5-z$.

Fig. 3. Ellipsoid plot (drawn at 30% probability level) of the asymmetric unit of **2** with partial atom labelling scheme. Intermolecular hydrogen-bond interactions are represented as dashed light-blue lines. Symmetry operation to generated equivalent atoms: i) $1/2-x, -y, -1/2+z$; ii) $1/2-x, -y, 1/2+z$; iii) $1/2-x, -1/2+y, z$.

Fig. 4. Ellipsoid plot (drawn at 30% probability level) of the asymmetric unit of **3** with partial atom labelling scheme. Intermolecular hydrogen-bond interactions are represented as dashed light-blue lines. Symmetry operation to generated equivalent atoms: i) $1-x, 1-y, 1-z$; ii) $2-x, -y, 1-z$.

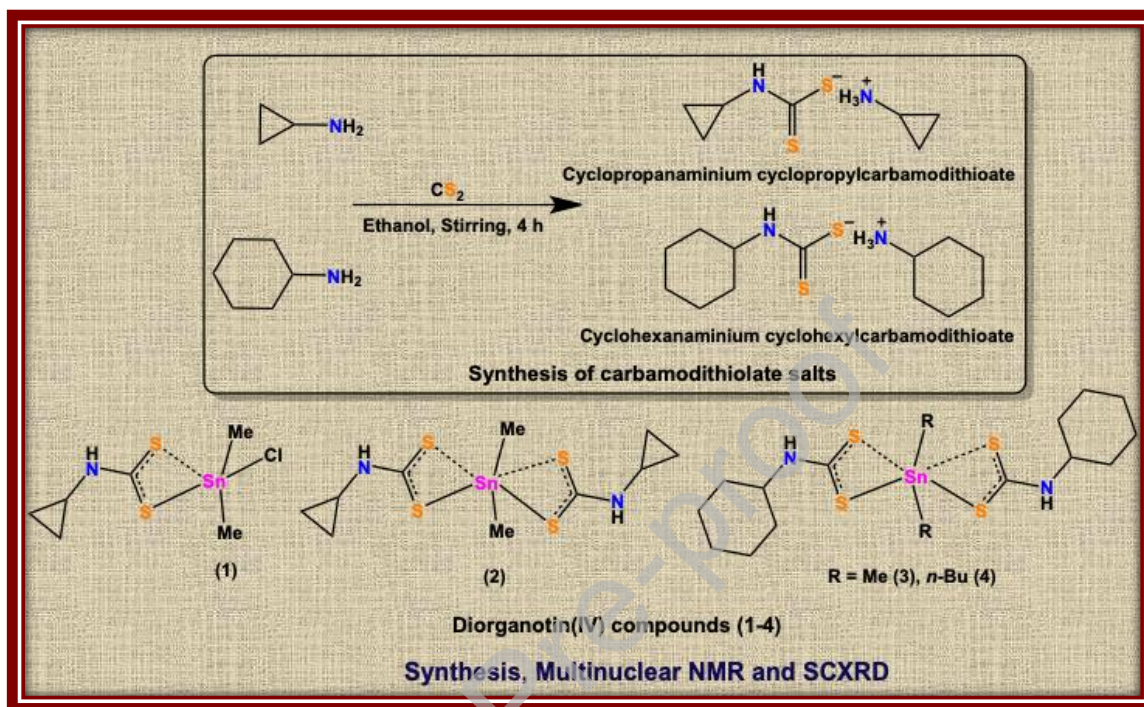
Fig. 5. Ellipsoid plot (drawn at 30% probability level) of the asymmetric unit of **4** with partial atom labeling scheme. Intermolecular hydrogen-bond interactions are represented as dashed light-blue lines. Symmetry operation to generated equivalent atoms: i) $1-x, 1-y, 1-z$; ii) $1-x, 2-y, 2-z$.

Fig. 6. Depiction of the d_{norm} Hirshfeld surfaces of the compounds in transparent mode.

Fig. 7. Fingerprint plots for the compounds with offset representations of the S...H contributions (also Cl...H for **1**) to the total Hirshfeld surfaces.

Fig. 8. Percentage contribution to the total Hirshfeld surface of the interactions in every compound (top), individual contributions of the molecules in **1** (middle), and of each ion in the dithiocarbamate salts (bottom).

Graphical Abstract



An efficient and highly practical method for the synthesis of cyclopropanaminium cyclopropylcarbamodithioate and cyclohexanaminium cyclohexylcarbamodithioate salts from their primary amine precursors is described. These salts produced **new** diorganotin(IV) dithiocarbamates upon reaction with diorganotin dihalide which uses a green process.